Baghdad Science Journal

Volume 23 | Issue 2 Article 22

2-24-2026

Continuum Discretized Coupled Channels Calculations for ^{6}He + ^{197}Au, ^{8}He + ^{197}Au and \ ^{11}Li + ^{208}Pb Neutron Halo Systems

Saddon Omran Gharib
Department of Physics, College of Education for Pure Sciences, University of Babylon, Iraq,
pure416.sadoon.omran@student.uobabylon.edu.iq

Fouad A. Majeed
Department of Physics, College of Education for Pure Sciences, University of Babylon, Iraq,
fmajeed@uobabylon.edu.iq

How to Cite this Article

Gharib, Saddon Omran and Majeed, Fouad A. (2026) "Continuum Discretized Coupled Channels Calculations for ^{6}He + ^{197}Au, ^{8}He + ^{197}Au and \ ^{11}Li + ^{208}Pb Neutron Halo Systems," *Baghdad Science Journal*: Vol. 23: Iss. 2, Article 22.
DOI: https://doi.org/10.21123/2411-7986.5214

BAGHDAD SCIENCE JOURNAL 2026;23(2):669–677

RESEARCH ARTICLE

Continuum Discretized Coupled Channels Calculations for ^{6}He + ^{197}Au, ^{8}He + ^{197}Au and ^{11}Li + ^{208}Pb Neutron Halo Systems

Saddon Omran Gharib *, **Fouad A. Majeed**

Department of Physics, College of Education for Pure Sciences, University of Babylon, Iraq

ABSTRACT

The difficulty in investigating fusion processes using neutron-rich halo nuclei resides in comprehending the system that allows the coupling between the elastic and breakup channels. The main objective of the present calculations is to identify the ideal coupling coefficient. that takes into account the effects of channel-coupling in computing the overall cross section of fusion section σ_{fus}, the distribution barrier of the fusion D_{fus}, and the probability P_{fus} for the subsequent systems ^{8}He + ^{197}Au,^{6}He + ^{197}Au, and ^{11}Li + ^{208}Pb, utilizing a quantum mechanical methodology. The coupled-channel (CC) code is used for doing quantum computations that include coupled channels. The quantum mechanical technique accurately agrees with the current observable data. Theoretical predictions of quantum mechanics exhibit exceptional agreement with the corresponding experimental results, especially in the area under the barrier of Coulomb.

Keywords: Channel-coupling, Fusion barrier distribution, Fusion cross section, Halo nuclei, Quantum tunneling

Introduction

One main goal of Low Energy Nuclear Physics (LENP) is to investigate the mechanisms by which loosely bound atomic nuclei collide at energies near stable or radioactive limits. A lot of work has been done, via theoretical and experimental investigations, to understand the many processes and crucial relationships during collision.[1] The occurrence of system rupture is essential in accidents that involve interconnected systems. Transfer pathways are of utmost importance, particularly for nuclei that are rich in neutrons and have elongated halos. The cross-sections for weakly bound systems display notable deviation as a result of their low threshold for breakup, and the breakup mechanism is highly effective in influencing other reaction pathways. Examining these events is essential in the area of astrophysics, as some reactions may function as significant routes for the formation of super-heavy materials.[2] The impact of two projectiles with weak couplings affects fusion due to the characteristics of the static fusion barrier differing from those of the fusion barrier for an identical target that has an isotope that is tightly bound. There are fewer obstacles because of the longer-density tail. It is generally accepted that this phenomenon greatly increases fusion cross-sections at energy around the sub-barrier. An essential consideration is how the elastic channel interacts with other channels, including breakdown, transition, and inelastic channels. It has been shown that fusion reactions at energies close to the sub-barrier, as measured by their cross-sections range are strongly enhanced by the existence of direct transfer channels and bound states undergoing inelastic excitations. On the other hand, the break-up technique has several features that define its continuum status, and there is disagreement within the continuum on the impact of ties to sources. The breakdown is still rather wide and the elastic channel shows a significant degree of coupling because of the weak binding. Apart from the standard transfer and inelastic channels, the cross-section can make a big difference.[2]

Received 19 February 2024; revised 22 November 2024; accepted 24 November 2024.
Available online 24 February 2026

* Corresponding author.
E-mail addresses: pure416.sadoon.omran@student.uobabylon.edu.iq (S. O. Gharib), fmajeed@uobabylon.edu.iq (F. A. Majeed).

https://doi.org/10.21123/2411-7986.5214

A comprehensive study of the channel coupling mechanism was using semiclassical and quantum mechanics.[3] The channel coupling is found very essential to be included when one of the partners of the fusion system is halo nucleus, due to the fact that weakly bound nucleons to the core nucleus make the breakup channel very important factor to be considered especially below the Coulomb barrier.[4] The semiclassical approach adopted to study the fusion reaction of weakly and stable systems is found to be very promising and compete with the calculations of the full quantum mechanical model. has been carried out by Majeed and his collaborators regarding the of study the fusion reaction of stable and halo systems by employing semiclassical and full quantum mechanical model. Yang et al. points out that, in the case of reactions with weakly bound nuclei around the Coulomb barrier, the fusion cross section is strongly affected by the couplings to the breakup and transfer channels. Their study indicates that theoretical methods like CDCC and coupled-channels calculations predict the experimental elastic scattering and fusion results fairly well.[5]

The continuum-discretized coupled-channels (CDCC) method has become a cornerstone in the theoretical description of breakup and transfer processes in deuteron- and halo-nucleus induced reactions, with developments ranging from the original formulation for three-body reaction models[6] to transfer-to-the-continuum approaches,[7] extensive methodological applications,[8] extensions including core excitation effects[9], and recent insights into breakup dynamics of exotic systems such as ^{11}Be and ^{6}He,[10,11] as well as modern coupled-channels perspectives covering exotic and superheavy nuclei[12] and current reviews of reaction dynamics in light exotic nuclei.[13]

This study aims to investigate the influence of the breakup of the channel-coupling on the theoretical calculations of the total fusion cross-section $\sigma_{fus}$the fusion barrier distribution $D_{fus}$and the probability P_{fus} for the systems ^{8}He + ^{197}Au,^{6}He + ^{197}Au, and ^{11}Li + ^{208}Pb, using the quantum mechanics with coupled channels to explore the heavy ion fusion reaction dynamics when the projectile is a halo nucleus. The coupled-channel (CC) code was used to carry out the computations, and the outcomes were compared with the previously observed data.

Background Theory

Fusion cross-section

The formulation of the essential equation for ascertaining fusion and elastic cross-sections is accomplished via a potential model with a single channel. It is possible to express the Schrodinger equation in three dimensions.[14]

$$\left[-\frac{\hbar^2}{2\mu}\nabla^2\phi\,(r)+V\,(r)\,\phi\,(r)-E\phi\,(r)\right]=0 \tag{1}$$

in which $[V(r)=V_C(r)+V_N(r)]$represents the overall potential, which is the sum of the contributions from the Coulomb and nuclear potentials, here μ is the reduced mass of the system.

The Woods-Saxon potential is considered the nuclear potential.[14]

$$V_n\,(r)=\frac{-V_0}{1+exp\left[\frac{r-R_n}{a_0}\right]} \tag{2}$$

where a_0 represents the potential diffuseness and V_0 denotes the depth of potential. The nuclear potential's radius R_n was expressed as follows:[14]

$$R_n=r_0\left[A_P^{\frac{1}{3}}+A_T^{\frac{1}{3}}\right] \tag{3}$$

The radius parameter is represented by the variable r_0.

The equation $\phi=\exp(i\vec{k}.\vec{r})$, $\vec{k}$ may be solved directly without taking into account the potential $\mathbb{v}(r)$ Here $k=\sqrt{2\mu E}/\hbar^2$provides the wave number vector magnitude. The form this solution takes asymptotically.[15]

$$\phi\,(r,\theta)=e^{i\vec{k}.\vec{r}}\rightarrow\frac{i}{2k}\sum_{l=0}^{\infty}(2l+1)\,i^l \left(\frac{e^{-ik(r-l\frac{\pi}{2})}}{r}-\frac{e^{ik(r-l\frac{\pi}{2})}}{r}\right)P_l\,(cos\theta)\,,\ r\rightarrow\infty \tag{4}$$

The vectors $\vec{k}$ and $\vec{r}$ form the angle θ, and $P_l$stands for the Legendre polynomials. The solution showed better behavior because of its potential. Eq. (2) may be used to define the shape of the wave function at infinity as the potential approaches zero as the distance approaches infinity. The analogous Coulomb waves will be used in place of the plane waves, yielding an asymptotic form of.[16]

$$\phi\,(r,\theta)\rightarrow\frac{i}{2k}\sum_{l=0}^{\infty}(2l+1)\,e^l \left(\frac{H_l^{(-)}(kr)}{r}-S_l\frac{H_l^{(+)}(kr)}{r}\right)P_l\,(cos\theta)\,,\ r\rightarrow\infty \tag{5}$$

The Coulomb outgoing and incoming waves are represented by the functions $H_l^{(-)}(kr)$and $H_l^{(+)}(kr)$,

respectively. S_ℓ is the nuclear S-Matrix a complicated word that is frequently difficult to calculate. Using the spherical harmonics as a foundation, the wave function $\phi(\vec{r})$is expanded in the S-matrix calculation. [16]

$$\phi\left(\vec{r}\right)=\sum_{l=0}^{\infty}\sum_{m=-l}^{l}A_{lm}\frac{u_l\left(r\right)}{r}Y_{lm}\left(\hat{r}\right) \tag{6}$$

The expansion coefficients for the Schrödinger equation that are fulfilled by $u_l(r)$are represented by the value of A_{lm}, which is. [17]

$$\left[-\frac{\hbar^2}{2\mu}\frac{d^2}{dr^2}+V\left(r\right)+\frac{l\left(l+1\right)\hbar^2}{2\mu r^2}-E\right]u_l\left(r\right)=0 \tag{7}$$

In order to tackle this problem, boundary conditions are used.

$$(r)\sim r^{l+1}\ r\to 0 \tag{8}$$

$$(r)=H_l^{(-)}\left(kr\right)-S_lH_l^{(+)}\left(kr\right)\ r\to\ \infty \tag{9}$$

Following the completion of the measurement of S_ℓ, the portion of the differential that is elastic in cross-section may be calculated to constitute. [17]

$$\frac{d\sigma_{el}}{d\Omega}=\left|f\left(\theta\right)\right|^2 \tag{10}$$

When

$$f\left(\theta\right)=\frac{i}{2k}\sum_{l=0}^{\infty}\left(2l+1\right)\left(1-S_l\right)\ P_l\left(cos\theta\right) \tag{11}$$

The entire cross-sectional value flexible is. [17]

$$\sigma_{el}=2\pi\int_{-1}^{1}d\left(cos\theta\right)\frac{d\sigma}{d\Omega}=\frac{\pi}{k^2}\sum_{l=0}^{\infty}\left(2l+1\right)\left|S_l-1\right|^2 \tag{12}$$

One way to define fusion reactions is as the absorption of incident flow. The absolute value of the s-matrix, represented by $|S|<1$ when the potentials are complex. We can calculate the disparity in overall radial flux among the waves that are entering and leaving using Eq. (3). [18]

$$j_{in}-j_{out}=\frac{k\hbar}{\mu}\frac{\pi}{k^2}\sum_{l}\left(2l+1\right)\left(1-\left|S_l\right|^2\right) \tag{13}$$

Through the process of integrating the radial flux over all possible values of θ and dividing it by the incident flux, $v=\hbar k/\mu$, Eq. (11) may be produced. After that, the value that was obtained is considered to be the fusion cross-section, which has the value of. [18]

$$\sigma_{fus}\left(E\right)=\frac{\pi}{k^2}\sum_{l}\left(2l+1\right)\left(1-\left|S_l\right|^2\right) \tag{14}$$

The conventional boundary condition at the origin is not applied in heavy-ion fusion. Eq. (8), known as the incoming wave boundary condition (IWBC), is employed to preserve the accuracy of the potential. Given this specific boundary condition, the wave function assumes a certain form and may be represented as. [18,19]

$$u_l\left(r\right)=\mathcal{T}_l exp\left(-i\int_{r_{abs}}^{r}k_l\left(r'\right)dr'\right)\ r\le r_{abs} \tag{15}$$

Inside the Coulomb barrier, the distance is less than the radius of absorption, which is represented as r_{abs}. The value of $k_l(r)$ is the l-th wave partial's local wave number, and it's equal to. [18]

$$k_l\left(r\right)=\sqrt{\frac{2\mu}{\hbar^2}\left(E-V\left(r\right)-\frac{l\left(l+1\right)\hbar^2}{2\mu r^2}\right)} \tag{16}$$

The substantial absorption inside the interior region gives rise to an incoming wave boundary condition, wherein the inflowing flow is not reflected. The ultimate outcomes of fusion of heavy-ion processes are not much affected by the absorption radius, r_{abs}as well as taking into account the potential's minimal position. Within the framework of IWBC, the symbol $\mathcal{T}_l$ in Eq. (13) denotes the transmission coefficient. Hence, the S-matrix represented as $S_l$in Eq. (7) corresponds to the reflection variable. Eq. (14) has undergone a transformation resulting in the creation of equation. [18,20]

$$\sigma_{fus}\left(E\right)=\frac{\pi}{k^2}\sum_{l}\left(2l+1\right)P_l\left(E\right) \tag{17}$$

Penetrability of the scattering process, more especially for the l -wave, is what is meant by the word $P_l(E)$ in this context. This penetrability is represented by the number. [19]

$$P_l\left(E\right)=1-\left|S_l\right|^2=\frac{k_l\left(r_{abs}\right)}{k}\left|\mathcal{T}_l\right|^2 \tag{18}$$

These boundary conditions are incorporated into Eqs. (6) and (13).

Table 1. Real and imaginary Akyüz-Winther potential parameters, height of Coulomb barrier and maximum angular momentum for studied fusion reactions.

Fusion reaction	V_0 (MeV)	r_0 (fm)	a_0 (fm)	W_0 (MeV)	r_i (fm)	a_i (fm)	V_b (MeV)	ℓ_{max}
^{8}He + ^{197}Au	63.0	1.200	0.500	21.0	0.938	0.777	19.20	64
^{6}He + ^{197}Au	237.9	1.000	0.700	79.3	0.929	0.783	19.2	70
^{11}Li + ^{208}Pb	50.3	0.980	0.540	16.8	0.952	0.769	35.2	46

The distribution of the fusion barrier

A mathematical portrayal of the classical cross-section of fusion is as follows:

$$\sigma_{fus}^{cl}(E) = \pi R_b^2 \left(1 - \frac{V_b}{E}\right) \theta(E - V_b) \tag{19}$$

The position of the barrier is shown by the sign R_b, while its height is indicated by V_b. The link between the center of mass's energy E and the cross-section of fusion σ_{fus}^{cl} may be found in the equation for the first derivative of the product, $d(E\sigma_{fus}^{cl}/dE)$ This derivative is comparable to a one-dimensional barrier of height $V_b$in classical mechanics in terms of penetrability.[20]

$$\frac{d}{dE}\left[E\sigma_{fus}^{cl}(E)\right] = \pi R_b^2\, \theta(E - V_b) = \pi R_b^2 P_{cl}(E) \tag{20}$$

The function's second derivative for delta.

$$\frac{d^2}{dE^2}\left[E\sigma_{fus}^{cl}(E)\right] = \pi R_b^2\, \delta(E - V_b) \tag{21}$$

In quantum physics, tunneling adds a widening effect to the delta function. An analytical technique called the Wong formula may be utilized to compute the cross-section of fusion. It approximates the Coulomb barrier by utilizing an inverted parabola.[20]

$$\sigma_{fus}(E) = R_b^2 \frac{\hbar\Omega}{2E}\, ln\left(1 + exp\left[\frac{2\pi}{\hbar\Omega}(E - V_b)\right]\right) \tag{22}$$

This is where the Coulomb curvature barrier is represented by the symbol $\hbar\Omega$. Based on the penetrability, the derivative of the first order of value $E\sigma_{fus}(E)$is measured to be.[21]

$$\frac{d}{dE}\left[E\sigma_{fus}^{cl}(E)\right] = \frac{\pi R_b^2}{1 + exp\left[-\frac{2\pi}{\hbar\Omega}(E - V_b)\right]} = \pi R_b^2\, P(E) \tag{23}$$

It is evident from this equation that there is a direct connection between the penetrability's first derivative and the cross-section, which is denoted by.[21]

$$\frac{d^2}{dE^2}\left[E\sigma_{fus}^{cl}(E)\right] = \pi R_b^2 \frac{2\pi}{\hbar\Omega} \frac{e^{-2\pi(E-V_b)/\hbar\Omega}}{\left(1 + e^{-2\pi(E-V_b)/\hbar\Omega}\right)^2} = \pi R_b^2 \frac{dP(E)}{dE} \tag{24}$$

Results and Discussion

In this section the calculations and the discussion of the study are presented for the studied systems ^{8}He + ^{197}Au,^{6}He + ^{197}Au, and ^{11}Li + ^{208}Pb. The calculations were performed using the coupled-channel (CC) code written in Fortran language for the two-channel model that includes the breakup channel. The estimated parameters for Akyüz-Winther potential were fitted and presented in Table 1 by using the least-squares fit technique.

Fig. 1: Using single and coupled channel formalism for quantum mechanical calculations, paneling (a), (b), and (c) compare the measured and calculated values of the cross-section of the reaction for the fusion σ_{fus}, the fusion probability P_{fus}, and the distribution barrier for the fusion $D_{fus}$for the system ^{8}He + ^{197}Au. The system ^{8}He + ^{197}Au experimental data is from.[22] There isn't much experimental data available for this system, but our theoretical calculations match the actual data, particularly for σ_{fus} and P_{fus}. As seen in Fig. 1 panel (b), coupled-channel computations are represented by a solid blue line that is displaced towards the smaller$E_{c.m.}$. axis and deviates from the Gaussian form. The position of the barrier height $V_b$is shown by the red arrows on the $E_{c.m.}$.axis. To improve the computations below the Coulomb barrier V_b, the channel coupling must be included.

This shift indicates that the inclusion of channel coupling effects results in a more accurate representation of the fusion barrier distribution, deviating from the simpler Gaussian shape often assumed in basic models. The red arrows on the $E_{c.m.}$axis indicate the precise location of the barrier height V_b. Channel coupling is essential for enhancing calculations performed below the Coulomb barrier V_b. where the electrostatic repulsion between nuclei plays a significant role. Including channel coupling in theoretical models ensures that these interactions are accurately

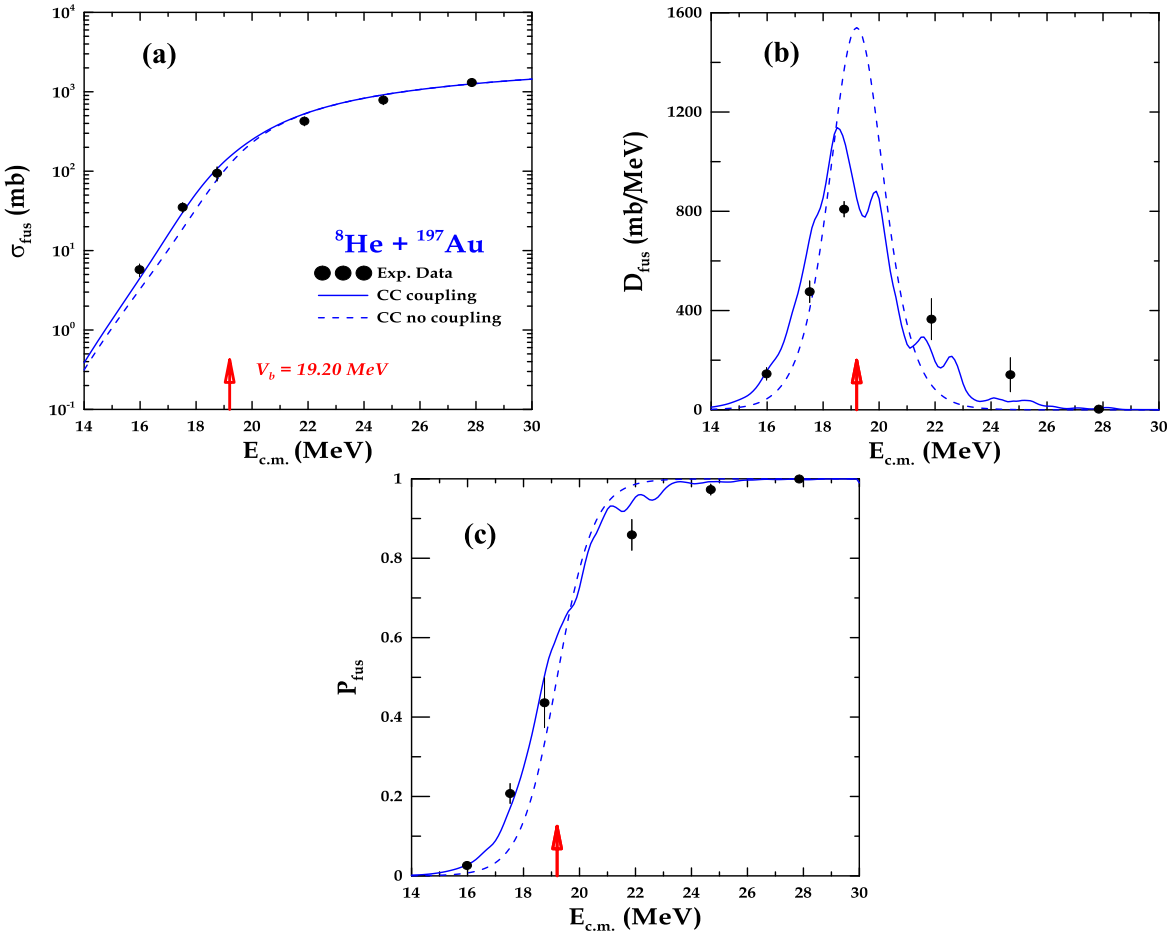

Fig. 1. Comparison of theoretical and observed data[22] for (a) cross-section of the fusion reaction σ_{fus} (b) Distribution of fusion barriers D_{fus}, and (c) Probability of fusion $P_{fus}$for the system ^{8}He + ^{197}Au. The red arrow refers to the position of the barrier height V_b.

represented, improving the predictive power of the models.

Fig. 2 panels (a), (b), and (c) illustrate the comparison concerning the estimated and observed values for the fusion reaction cross-section σ_{fus}, the distribution barrier of the fusion D_{fus}, and fusion probability P_{fus}, respectively. The computations were conducted utilizing quantum mechanical techniques and employing both single and linked channel formalism. The available experimental data[23] for this system are restricted, but our theoretical calculations were compatible with the actual data, notably for the parameters $\sigma_{fus}$and P_{fus}. The coupled- channel calculations exhibit a downward shift along the $E_{c.m.}$ axis and a departure from the Gaussian form, as seen by the dashed blue line in Fig. 2 panel (b). The red arrow located at the $E_{c.m.}$ axis indicates the precise location of the barrier height V_b. Channel coupling is essential for enhancing calculations performed below the Coulomb barrier V_b. The results also reveal that the fusion barrier distribution is non-Gaussian when channel coupling is considered, shifting towards lower energies on the $E_{c.m.}$ axis

Fig. 3 depicts in panels (a, b and c) the comparison between the estimated and observed cross-section of the fusion reaction σ_{fus}, the distribution barrier of the fusion D_{fus}, and the fusion probability P_{fus}, respectively, for ^{11}Li + ^{208}Pb system. The comparisons were conducted using quantum mechanical computations, utilizing both single and linked channel formalism. The empirical data[24] for the ^{11}Li + ^{208}Pb system was acquired from the referenced source. The dataset available for this system is constrained, but, our theoretical computations shown a high degree of agreement with the empirical data, notably with the variables $\sigma_{fus}$and P_{fus}. The linked channel calculations exhibit a downward shift along the $E_{c.m.}$ axis and a departure from the Gaussian form, as seen by the dashed blue line in Fig. 3 panel (b). The position of the barrier height V_b is shown by the red arrows on the $E_{c.m.}$ axis. Channel coupling is essential for enhancing calculations conducted below the Coulomb barrier V_b.

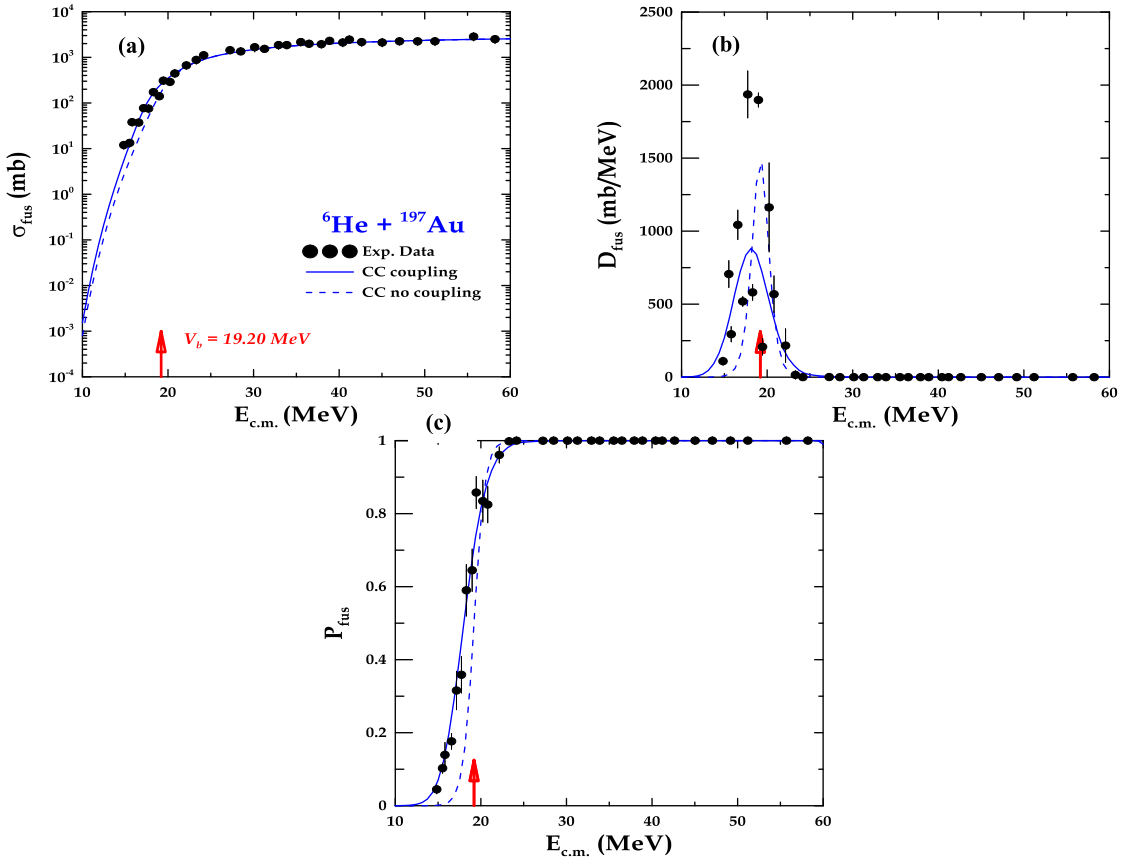

Fig. 2. Presents a comparison between the theoretical and observed results[23] for the cross-section of the fusion reaction σ_{fus}, distribution of fusion barrier D_{fus}, and probability of fusion $Pfus$ for the ^{6}He + ^{197}Au system. The red arrow refers to the position of the barrier height V_b.

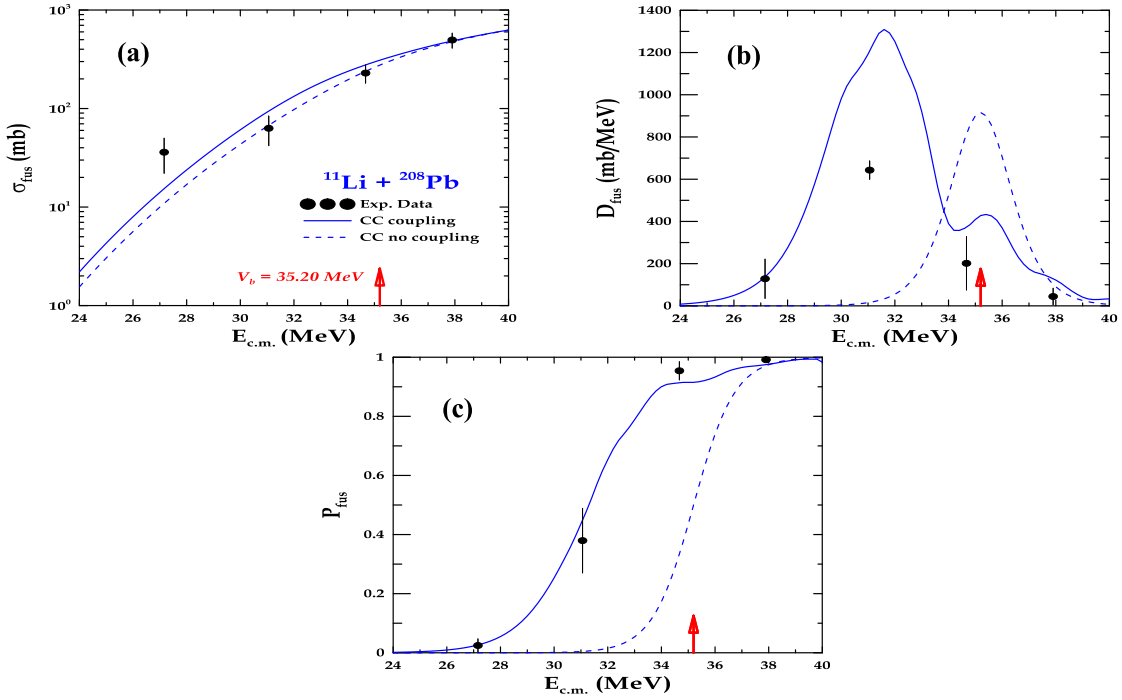

Fig. 3. A comparison between theoretical and observed data[24] for the system ^{11}Li + ^{208}Pb shows the (a) cross section of fusion reaction σ_{fus}, (b) the distribution barrier of the fusion D_{fus}, and (c) probability of the fusion P_{fus}. The red arrow refers to the position of the barrier height V_b.

At lower energies, coupling effects can significantly influence the reaction outcome, leading to deviations between predicted and observed results. However, as the energy increases, the influence of coupling effects may diminish, and the fusion process becomes more dominated by the elastic channel.

The neutrons in the halo can increase the likelihood of a nuclear reaction at lower energies, as they can easily separate from the core. This alters the reaction behavior compared to nuclei without a halo, leading to higher reaction probabilities at lower energies.

Conclusion

The work conducted a comprehensive theoretical evaluation of the computations for σ_{fus}, D_{fus}, and $P_{fus}$for the ^{8}He + ^{197}Au,^{6}He + ^{197}Au, and ^{11}Li + ^{208}Pb systems. The appropriate coupling parameters were obtained by applying the Woods-Saxon parameters that best suit the observed and computed barrier height V_b, aligning with its centroid. The comparison between the conclusions and the experimental data highlights the crucial significance of the breakup channel in providing an accurate description of the fusion cross-section (σ_{fus}), fusion barrier distribution (D_{fus}), and the Probability (P_{fus}) for systems utilizing light halo nuclei as a projectile. Theoretical simulations of quantum mechanics provide a satisfactory level of concordance with the existing observable data upon comparison. The results of this work are of great significance for scientists who are explicitly investigating the physics of weakly bound systems, particularly those in which the target of motion is a halo nucleus. This work can be extended to explore further additive combinations of halo nuclei with other target nuclei to augment the knowledge of fusion dynamics for more diverse mass numbers and nuclear shapes.

Acknowledgment

The authors express their gratitude to the Department of Physics at the University of Babylon's College of Education for Pure Sciences. for making this task easier.

Authors' declaration

- Conflicts of Interest: None.
- We hereby confirm that all the Figures and Tables in the manuscript are ours. Furthermore, any Figures and images, that are not ours, have been included with the necessary permission for republication, which is attached to the manuscript.
- No animal studies are present in the manuscript.
- No human studies are present in the manuscript.
- Ethical Clearance: The project was approved by the local ethical committee at University of Babylon.

Authors' contribution statement

Authors S. O. collected the experimental data, performed the calculations and contributed to the discussion and conclusion sections. The author F. A. M. wrote the introduction section, theory section and contributed partially in the discussion section and the conclusion section. All authors contributed equally in preparing the manuscript.

References

1. Pakou A, Sgouros O, Soukeras V, Casal J, Rusek K. Reaction mechanisms of the weakly bound nuclei ^{6,7}Li and ^{7,9}Be on light targets at near barrier energies, Eur Phys J A. 2022 Jan;58(8):8-58. https://doi.org/10.1140/epja/s10050-021-00655-w.
2. Mohr P. Total reaction cross section of light stable and exotic nuclei on lead at energies around the Coulomb barrier. Eur Phys J A. 2024 Sep;60(9):1–35. https://doi.org/10.1140/epja/s10050-024-01403-6.
3. Majeed FA, The role of the breakup channel on the fusion reaction of light and weakly bound nuclei, Int J Nucl Energ Sci Tech. 2017 Nov;11:218–228. https://doi.org/10.1504/IJNEST.2017.088068.
4. Khuadher MA, Majeed FA. The Effect of the Proton and Neutron as Probe for the Nuclear Fusion Reactions at Near-Barrier Energies. East Euro J Phys. 2023 Sep;4(3):178–86. https://doi.org/10.26565/2312-4334-2023-3-14.
5. Yang L, Lin CJ, Ma NR, Wen PW, Jia HM, Yang F. Breakup dynamics of weakly bound nuclei at energies around the Coulomb barrier. Fundamental Research. 2023 Nov 8:2463–2473. https://doi.org/10.1016/j.fmre.2023.10.006.
6. Austern N, Iseri Y, Vincent CM, Yahiro M. Continuum-discretized coupled-channels calculations for three-body models of deuteron-nucleus reactions. Phys Rep. 1987;154:125–204. https://doi.org/10.1016/0370-1573(87)90094-9.
7. Moro AM, Nunes FM. Transfer to the continuum and breakup reactions. Nucl Phys A. 2006;767:138–154. https://doi.org/10.1016/j.nuclphysa.2005.12.016.
8. Yahiro M, Ogata K, Matsumoto T, Minomo K. The continuum-discretized coupled-channels method and its applications. Prog Theor Exp Phys. 2012;2012(1):01A206. https://doi.org/10.1093/ptep/pts008.
9. De Diego R, Arias JM, Lay JA, Moro AM. Continuum-discretized coupled-channels calculations with core excitation. Phys Rev C. 2014;89:064609. https://doi.org/10.1103/PhysRevC.89.064609.
10. Di Pietro A, Moro AM, Lei J, de Diego R. Insights into the dynamics of breakup of the halo nucleus ^{11}Be on a ^{64}Zn target. Physics Letters B. 2019 Nov 10;798:134954. https://doi.org/10.1016/j.physletb.2019.134954.

11. Escrig D, Sanchez-Benitez AM, Moro AM, Alvarez MA, Andres MV, Angulo C, Borge MJ, Cabrera J, Cherubini S, Demaret P, Espino JM. α-particle production in the scattering of ^{6}He by ^{208}Pb at energies around the Coulomb barrier.. Nucl Phys A. 2007;792:2–19. https://doi.org/10.1016/j.nuclphysa.2007.05.012.
12. Hagino K, Ogata K, Moro AM. Coupled-channels calculations for nuclear reactions: From exotic nuclei to superheavy elements. Progress in Particle and Nuclear Physics. 2022 Jul 1;125:103951. https://doi.org/10.1016/j.ppnp.2022.103951.
13. Di Pietro A. Reaction dynamics and nuclear structure of light exotic nuclei. InEPJ Web of Conferences 2024 (Vol. 311, p. 00014). EDP Sciences. https://doi.org/10.1051/epjconf/202431100014.
14. Canto LF, Gomes PRS, Donangelo R, Hussein MS. Fusion and breakup of weakly bound nuclei. Phys Rep. 2006 Feb;424:1–111. https://doi.org/10.1016/j.physrep.2005.10.006.
15. Blinder SM. Introduction to quantum mechanics. Academic Press;2020 Oct 9. https://doi.org/10.1016/C2019-0-04431-7.
16. Sakurai JJ, Napolitano J. Modern Quantum Mechanics. Cambridge University Press;3rd edition;2020. https://doi.org/10.1017/9781108587280.
17. Tanihata I, Toki H, Kajino T, editors. Handbook of nuclear physics. Springer Nature;2023 Sep 4. https://doi.org/10.1007/978-981-19-6345-2.
18. Hebborn C, Capel P. Halo effective field theory analysis of one-neutron knockout reactions of ^{11}Be and ^{15}C. Phys Rev C. 2021 Aug;104(2):024616. https://doi.org/10.1103/PhysRevC.104.02461.
19. Abbas SA, Hussein AA, Obaid SM, Mohammed NA. Fusion Reaction Study of some Selected Halo Systems. Baghdad Science Journal. 2023;20(2):18. https://doi.org/10.21123/bsj.2022.6985.
20. Ferreira JL, Rangel J, Lubian J, Canto LF. Fusion reactions in collisions of neutron halo nuclei with heavy targets. Physical Review C. 2023 Mar;107(3):034603. https://doi.org/10.1103/PhysRevC.107.034603.
21. Palli K, Pakou A, Moro AM, O'Malley PD, Acosta L, Sánchez-Benítez AM, Souliotis G, Aguilera EF, Andrade E, Godos D, Sgouros O. Quasielastic scattering of ^{7}Be+ ^{nat}Zr at sub-and near-barrier energies. Phys Rev C. 2023 Jun;107(6):064613. https://doi.org/10.1103/PhysRevC.107.064613.
22. Lemasson A, Shrivastava A, Navin A, Rejmund M, Keeley N, Zelevinsky V, *et al.* Modern Rutherford experiment: Tunneling of the most neutron-rich nucleus. Phys Rev Lett. 2009 Dec 4;103(23):232701. https://doi.org/10.1103/PhysRevLett.103.232701.
23. Deb NK, Kalita K, Rashid HA, Nath S, Gehlot J, Madhavan N, *et al.* Role of neutron transfer in the sub-barrier fusion cross section in ^{18}O+ ^{116}S. Phys Rev C. 2020 Sep;102(3):034603. https://doi.org/10.1103/PhysRevC.102.034603.
24. Azhib AK, Samarin VV, Kuterbekov KA. Neutron transfer and nuclear breakup in ^{208}Pb (^{11}Li, ^{9}Li) reaction. 2020;4(1):19–28. https://doi.org/10.29317/ejpfm.2020040103.

حساب القنوات المترابطة المتقطعة لأنظمة نوى الهالة النيوترونية $^{11}Li + ^{208}Pb$ و $^{8}He + ^{197}Au, ^{6}He + ^{197}Au,$

سعدون عمران غريب، فؤاد عطية مجيد

قسم الفيزياء، كلية التربية للعلوم الصرفة، جامعة بابل، بابل، العراق.

الخلاصة

تكمن الصعوبة في دراسة عمليات الاندماج باستخدام نوى الهالة الغنية بالنيوترونات في فهم النظام الذي يسمح بالاقتران بين القنوات المرنة وقنوات الانفصال. الهدف الرئيسي من الحسابات الحالية هو تحديد معامل الاقتران المثالي الذي يأخذ في الاعتبار تأثيرات اقتران القناة في حساب المقطع العرضي للأندماج الكلي σ_{fus}، وحاجز توزيع الاندماج D_{fus}، واحتمالية الأندماج P_{fus} للأنظمة اللاحقة $^{8}He + ^{197}Au, ^{6}He + ^{197}Au,$ و $^{11}Li + ^{208}Pb$ ، باستخدام منهجية ميكانيكا الكم. تم استخدام برنامج القناة المزدوجة (CC) لإجراء الحسابات الكمومية التي تتضمن القنوات المزدوجة. تتوافق تقنية ميكانيكا الكم بدقة مع البيانات الحالية التي يمكن ملاحظتها. تظهر التنبؤات النظرية لميكانيكا الكم توافقًا استثنائيًا مع النتائج التجريبية المقابلة، خاصة في المنطقة الواقعة تحت حاجز كولومب.

الكلمات المفتاحية: القنوات المزدوجة، توزيع حواجز الاندماج، المقطع العرضي للاندماج، النوى ذات الانظمة الهالية. النفق الكمي.